Progress In Electromagnetics Research M, Vol. 70, 177–185, 2018

Investigating the Impacts of Meteorological Parameters on Electromagnetic Environment of Overhead Transmission Line

Yang Mo[1], Yanling Wang[1, *], Fan Song[1], Zheng Xu[2], Qiang Zhang[3], and Zhiqiang Niu[4]

Abstract—The meteorological parameters along the overhead line change significantly, which have an effect on the surrounding electromagnetic environment. The analysis method of meteorological parameters impacting the electromagnetic environment is presented in this paper. Firstly, the conductor temperature is solved iteratively by the heat balance equation. Secondly, the power flow model involving the conductor temperature is established based on the relationship between line parameters and conductor temperature. Finally, the electromagnetic environment surrounding the line is analyzed based on the changes of line voltage and current. In the case study, the electromagnetic environment of the IEEE 5-bus system under the three cases is analyzed and compared. It is proved that the changes of meteorological parameters along the line have an important impact on the surrounding electromagnetic environment. The calculation of electromagnetic environment considering the changes of meteorological parameters is more accurate.

1. INTRODUCTION

With the increasing awareness of environmental protection in the society, the electromagnetic environment of transmission lines is getting more and more attention. The analysis of electromagnetic environment such as electric field effect, magnetic field effect and radio interference has become one of the key issues in the design of transmission lines [1]. There are a lot of literatures on the analysis of electromagnetic environment around transmission lines. In [2], the harm of electromagnetic environment of transmission lines to human body is analyzed. In [3], the theoretical values of electromagnetic environment indicators for ultra high voltage alternating current transmission lines are obtained by calculation method. In [4], the theoretical values of electromagnetic environment indicators of high voltage direct current transmission lines are calculated by calculation method. However, in these articles, the meteorological parameters along the lines are set as constant values, and the impact of meteorological parameters on the electromagnetic environment is neglected.

In fact, there are significant variations in the meteorological conditions along the transmission lines. In [5], meteorological data for 7 years is provided by the Shandong University (Weihai) Observatory. In the data, the highest ambient temperature is 42°C, the lowest ambient temperature is −13.5°C, and the highest wind speed is 22.7 m/s. There are significant variations in the ambient temperature and wind speed. The conductor temperature of transmission line is determined by the line current and meteorological parameters [6]. In [7], the conservative meteorological data is used by traditional static thermal rating to determine the operation limits of the line. For example, wind speed is designed to be 0.5 m/s, and ambient temperature is designed to be 40°C. In [8], seasonal thermal rating is studied, and the operation limits are determined based on the meteorological data from different seasons. In [9], the

Received 14 June 2018, Accepted 12 July 2018, Scheduled 20 July 2018

* Corresponding author: Yanling Wang (wangyanling@sdu.edu.cn).

[1] School of Mechanical, Electrical and Information Engineering, Shandong University (Weihai), Weihai, Shandong 264200, China. [2] State Grid Shandong Electric Power Company, Jinan, Shandong 250001, China. [3] Shandong Electric Power Dispatching Control Center, Jinan, Shandong 250000, China. [4] State Grid Weihai Power Supply Company, Weihai, Shandong 264200, China.

real-time changes in meteorological conditions are taken into account by dynamic thermal rating, and the accuracy of the calculation result is improved.

The real-time changes in meteorological conditions impact the conductor temperature and ultimately impact the system power flow. In [10], it is proved that the variation of wind speed along the line has a significant impact on the system power flow. In [11], it is proved that the temporal-spatial variation of meteorological parameters has a significant impact on the conductor temperature, and ultimately has a significant impact on the system power flow. The system power flow includes the current and voltage of the line. The variation of line voltage will impact the power frequency electric field and radio interference, and the variation of line current will impact the power frequency magnetic field [12].

In this paper, the variations of meteorological parameters along the lines are considered, and the analysis method of meteorological parameters impacting the electromagnetic environment is presented. Firstly, the conductor temperature is solved iteratively by the heat balance equation. Secondly, the relationship between line parameters and conductor temperature is presented, and the power flow model involving the conductor temperature is established. Finally, the electromagnetic environment around the line is analyzed based on the changes of line voltage and current. The power flow and electromagnetic environment of the IEEE 5-bus system under three cases are analyzed and compared. It is proved that the changes of meteorological parameters along the line have an important impact on the surrounding electromagnetic environment. The calculation of electromagnetic environment considering the changes of meteorological parameters is more accurate.

2. METHOD AND MODEL

2.1. Line Conductor Temperature Calculation

The conductor temperature of transmission lines is determined by its current and surrounding meteorological parameters, such as ambient temperature, wind speed and wind direction. When the current and the meteorological parameters are constants, the heat absorption and heat dissipation will be in equilibrium state. In the CIGRE standard [13], the heat balance equation is shown in Eq. (1):

$$q_{\mathrm{s}} + I^2 r = q_{\mathrm{r}} + q_{\mathrm{c}} \tag{1}$$

where q_{s} is the absorption heat from solar radiation, mainly influenced by the sun radiation angle; I is the current; r is the conductor resistance; q_{r} is the radiation heat loss, mainly influenced by the conductor temperature and ambient temperature; q_{c} is the convection heat loss, mainly influenced by the conductor temperature, ambient temperature, wind speed and wind direction.

The heat balance equation is an implicit function of the conductor temperature. It is necessary to set the initial value and iteratively solve the equation. When the result is stabilized gradually, the final value is conductor temperature value.

2.2. Relationship Between Line Parameters and Conductor Temperature

There are four main parameters for overhead transmission lines: series resistance r, series reactance x, shunt susceptance b and shunt conductance g. These parameters depend on the material characteristics of the conductor and the geographical location of the lines [14]. The conductor resistance and reactance are related to the conductor temperature, as shown in Eqs. (2) and (3):

$$r(T_{\mathrm{c}}) = r(T_0) \cdot [1 + \alpha(T_{\mathrm{c}} - T_0)] \tag{2}$$

$$x(T_{\mathrm{c}}) = x(T_0) \cdot [1 + \beta(T_{\mathrm{c}} - T_0)] \tag{3}$$

where T_0 is the reference temperature, usually taken as 20°C; T_{c} is the conductor temperature; α is the temperature coefficient of resistance, determined by the physical properties of the conductor [15]; β is the temperature coefficient of reactance.

2.3. Power Flow Model

Transmission line is the main component of power system. The changes of line parameters will affect the system power flow. The line power and current are calculated by Eqs. (4) and (5):

$$\left.\begin{aligned} P_{ij} &= V_i^2 r_{ij} / \left(r_{ij}^2 + x_{ij}^2\right) - V_i V_j / \left(r_{ij}^2 + x_{ij}^2\right) \left[r_{ij}\cos\delta_{ij} + x_{ij}\sin\delta_{ij}\right] \\ Q_{ij} &= -V_i^2 x_{ij} / \left(r_{ij}^2 + x_{ij}^2\right) - V_i V_j / \left(r_{ij}^2 + x_{ij}^2\right) \left[r_{ij}\sin\delta_{ij} - x_{ij}\cos\delta_{ij}\right] \end{aligned}\right\} \tag{4}$$

$$I_{ij} = \frac{\sqrt{P_{ij}^2 + Q_{ij}^2}}{V_i} \tag{5}$$

where i and j are the buses at both ends of the line; V_i and V_j are the voltage amplitude of bus i and bus j; $\delta_{ij} = \delta_i - \delta_j$ is the voltage phase angle difference between bus i and bus j; r_{ij} and x_{ij} are the resistance and reactance between bus i and bus j, related to the conductor temperature. It can be seen that the change of the conductor temperature will directly affect the system power flow.

2.4. Electromagnetic Environment Analysis

In the electromagnetic environment analysis of alternating current transmission lines, four indicators are considered: power frequency electric field, power frequency magnetic field, radio interference and audible noise [16]. The electric field intensity at point $P(x, y)$ can be calculated by Eqs. (6) and (7):

$$[Q_{\mathrm{c}}] = [C]^{-1}[U] \tag{6}$$

$$\left.\begin{aligned} E_{\mathrm{x}} &= \frac{1}{2\pi\varepsilon}\sum_{k=1}^{n} Q_{ck}\left(\frac{x - x_k}{d_k^2} - \frac{x - x_k}{d_k'^2}\right) \\ E_{\mathrm{y}} &= \frac{1}{2\pi\varepsilon}\sum_{k=1}^{n} Q_{ck}\left(\frac{y - y_k}{d_k^2} - \frac{y - y_k}{d_k'^2}\right) \end{aligned}\right\} \tag{7}$$

where $[Q_{\mathrm{c}}]$ and $[U]$ are the charge and voltage matrices, respectively; E_{x} and E_{y} are the abscissa and ordinate components of electric field intensity, respectively; ε is the air dielectric constant; k is the line number; n is the sum of the number of lines and the number of mirror lines; x_k and y_k are the abscissa and ordinate of the line k; d_k and $d_k^{'}$ are the distance from the point $P(x, y)$ to the line k and its mirror line, respectively; $[C]$ is the potential coefficient matrix, and the potential coefficients are obtained by Eq. (8):

$$\left.\begin{aligned} C_{m,m} &= \frac{1}{2\pi\varepsilon}\ln\frac{2H}{R} \\ C_{m,n} &= \frac{1}{2\pi\varepsilon}\ln\frac{D_{m,n}{}'}{D_{m,n}} \\ C_{m,n} &= C_{n,m} \end{aligned}\right\} \tag{8}$$

where H is the vertical distance from the line to ground; R is the line radius; $D_{m,n}$ and $D_{m,n}{}'$ are the distance from the line m to the line n and its mirror line, respectively. According to $E = \sqrt{E_{\mathrm{x}}^2 + E_{\mathrm{y}}^2}$, electric field intensity can be obtained. It can be seen that the change of the line voltage will directly affect the power frequency electric field.

According to the ampere circuit theorem, the magnetic field intensity at point $P(x, y)$ can be calculated by Eq. (9):

$$\left.\begin{aligned} M_{\mathrm{x}} &= \sum_{k=1}^{n} \frac{\mu I_k}{2\pi}\left(\frac{x_k - x}{d_k^2}\right) \\ M_{\mathrm{y}} &= \sum_{k=1}^{n} \frac{\mu I_k}{2\pi}\left(\frac{y_k - y}{d_k^2}\right) \end{aligned}\right\} \tag{9}$$

where μ is the magnetic permeability; I_k is the current of the line k; M_x and M_y are the abscissa and ordinate components of magnetic field intensity, respectively. According to $M = \sqrt{M_x^2 + M_y^2}$, magnetic field intensity can be obtained. It can be seen that the change of the line current will directly affect the power frequency magnetic field.

The engineering method recommended by the International Special Committee on Radio Interference (CISPR) is used to obtain the radio interference. The radio interference E_{RI} at the point, 20 m away from the side line and 2 m above the ground, can be calculated by Eq. (10):

$$E_{\mathrm{RI}} = 1.75Q_c/\pi\varepsilon R + 12R - 30 - 33\lg(d/20) \tag{10}$$

where d is the distance from the line; Q_c is the charge of the line, mainly influenced by the voltage according to Eq. (6). It can be seen that the change of the line voltage will directly affect the radio interference.

3. CASE STUDY

In this paper, an improved 5-bus power system is taken as the example. The network structure is shown in Figure 1. The voltage level is 220 kV, and the transmission line type is LGJ-400/50, whose section area of aluminum is 399.73 mm^2. The conductor diameter is 27.63 mm. The phase sequence is horizontal arrangement, and the spacing is 8 m. The height of the line to ground is 10 m. Parameter settings are as follows: the resistance is 0.07875 Ω/km at 20°C; the reactance is 0.4295 Ω/km at 20°C; the susceptance is 2.6471×10^{-6} S/km; the resistance and reactance temperature coefficients are both 0.0039 (1/°C). The length of branch 1–2 is 120 km, and the lengths of branches 2–3 and 1–3 are both 300 km. The power flow and electromagnetic environment indicators at the midpoint of the three branches are calculated and analyzed. The positions of the calculation points A, B, and C are shown in Figure 1.

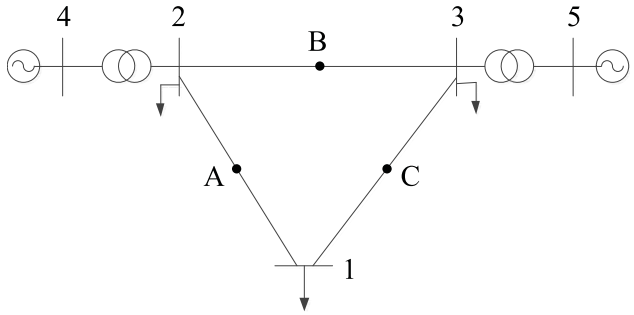

Figure 1. Network structure diagram.

In this paper, the 8784 hours of meteorological data in 2016 are provided by the Shandong University (Weihai) Observatory. The data at two typical moments is selected as case 1 and case 2, as shown in Table 1. Case 1 is at 17 o'clock on January 22, 2016. This moment is in winter, and the weather is cold and windy. The transmission environment is comfortable. Case 2 is at 9 o'clock on July 13, 2016. This moment is in summer, and the weather is hot and less windy. The transmission environment is bad. As can be seen from Table 1, the temperature difference between the two cases is 47.6°C, and the wind speed difference is 12.2 m/s. There are significant changes in meteorological parameters.

Table 1. Meteorological data of the two cases.

Case	Time	Ambient temperature (°C)	Wind Speed (m/s)
Case 1	17 o'clock on January 22, 2016	−13.4	12.4
Case 2	9 o'clock on July 13, 2016	34.2	0.2

In the conventional analysis and calculation of power system, the changes of weather conditions along the transmission line are not considered, and the conductor temperatures of all transmission lines are 20°C. This case is set as the base case.

3.1. Power Flow Analysis

Based on the meteorological data, the results of the system power flow of the three cases are obtained. The conductor temperature and line parameters of the branch 1–3 are shown in Table 2. For the conductor temperature, case 1 is the lowest, which is −10.33°C. Case 2 is the highest, which is 60.25°C. The difference of conductor temperature is 70.58°C. It can be seen that the meteorological parameters have a significant effect on the conductor temperature.

Table 2. Conductor temperature and line parameters of branchs 1–3.

Case	Conductor temperature (°C)	r (p.u.)	x (p.u.)	b (p.u.)
Base case	20	0.0488	0.2662	0.3782
Case 1	−10.33	0.0430	0.2348	0.3782
Case 2	60.25	0.0564	0.3080	0.3782

For the line resistance r, case 1 is the lowest, which is 0.043 p.u. Case 2 is the highest, which is 0.0564 p.u. The difference of line resistance is 0.0126 p.u.. For the line reactance x, case 1 is the lowest, which is 0.2348 p.u.. Case 2 is the highest, which is 0.308 p.u. The difference of line reactance is 0.0732 p.u. It can be seen that the conductor temperature has a significant effect on the line parameters.

The calculation results of current and voltage are shown in Table 3. Under the three cases, the change in current at point B is most obvious. Case 1 is 358.82 A, which is 4.25% lower than base case. Case 2 is 415.87 A, which is 10.97% higher than base case. The difference between case 1 and case 2 is 57.05 A. Under the three cases, the change in voltage at point C is most obvious. Case 1 is 0.97 p.u., which is 2.11% higher than base case. Case 2 is 0.89 p.u., which is 6.32% lower than base case. The difference between case 1 and case 2 is 0.08 p.u. It can be seen that the meteorological parameters have a great influence on the current and voltage of the line.

Table 3. System power flow results.

Case	Current I (A)			Voltage magnitude $\|V\|$ (p.u.)		
	A	B	C	A	B	C
Base case	160.98	374.76	582.12	1.04	0.96	0.95
Case 1	161.06	358.82	568.30	1.04	0.97	0.97
Difference	0.05%	4.25%	2.37%	0	1.04%	2.11%
Case 2	176.10	415.87	648.93	1.02	0.89	0.89
Difference	9.39%	10.97%	11.48%	1.92%	7.29%	6.32%

3.2. Power Frequency Electric Field Analysis

The height of calculation point to ground is 1.5 m. The horizontal range is between $-20 \sim +20$ m. The electric field intensity is calculated every 0.01 m horizontal distance. The electric field intensity distribution curves at three points are shown in Figure 2.

The distribution curve of the electric field intensity is bimodal distribution because of the horizontal arrangement of phase sequences. The maximum electric field intensity E_{m} occurs in the position 9 m far from the center of the tower. Overall, for the electric field intensity, case 1 is higher than base case, and

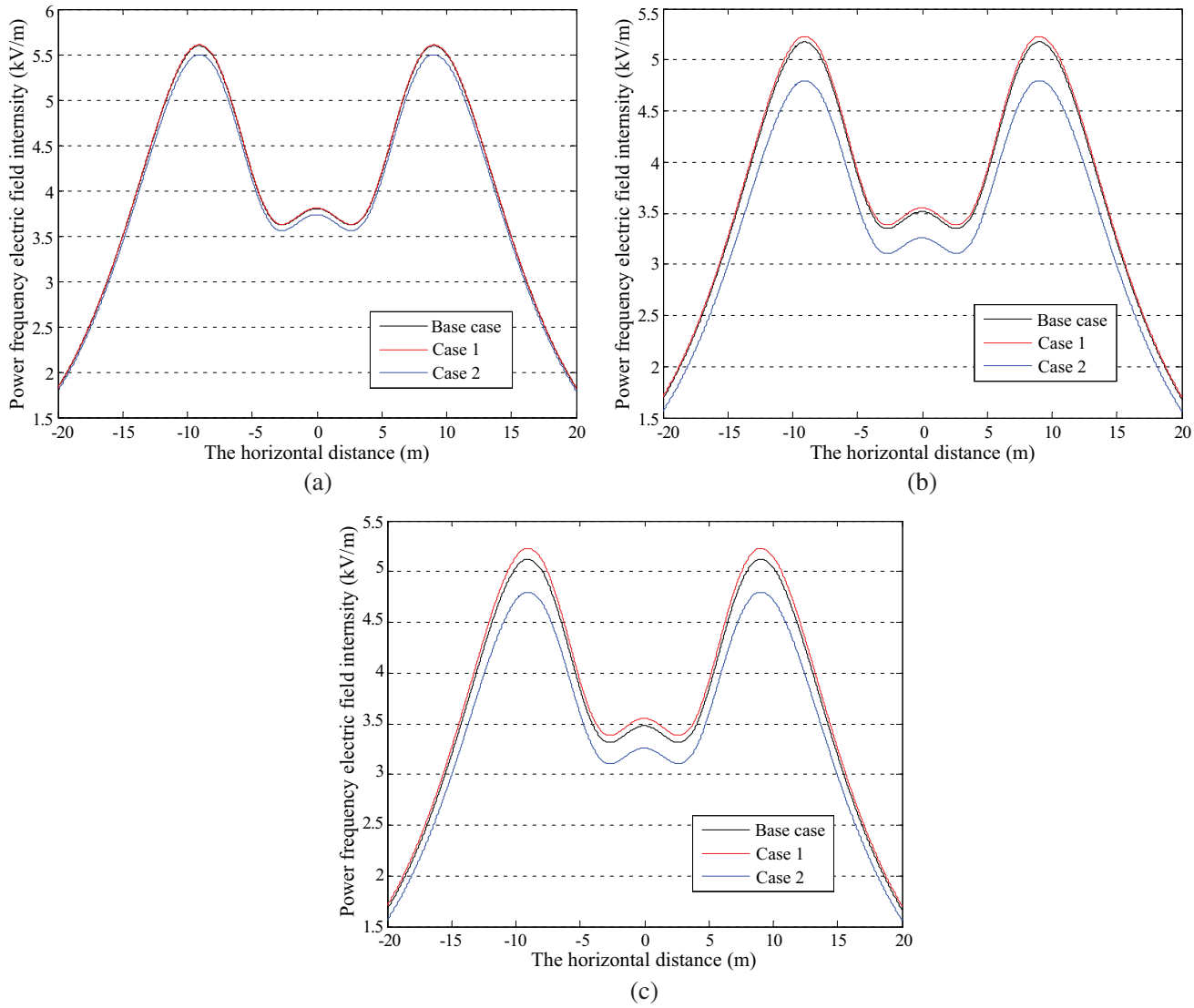

Figure 2. Power frequency electric field: (a) point A; (b) point B; (c) point C.

case 2 is lower than base case. The closer to the tower, the more obvious the phenomenon. The profile width where electric field intensity is higher than 4 kV/m is taken as the corridor width CW [17]. The CW and E_{m} under the three cases are shown in Table 4.

Table 4. E_{m} and CW under the three cases.

	Position	Base case	Case 1	Difference	Case 2	Difference
E_{m} (kV/m)	A	5.61	5.61	0	5.50	1.96 %
	B	5.18	5.23	0.97%	4.80	7.34%
	C	5.12	5.23	2.15%	4.80	6.25%
CW (m)	A	27.76	27.76	0	27.44	1.15%
	B	26.34	26.54	0.76%	24.86	5.62%
	C	26.14	26.54	1.53%	24.86	4.90%

The change in E_{m} at point C is most obvious. Case 1 is 5.23 kV/m, which is 2.15% higher than base case. Case 2 is 4.8 kV/m, which is 6.25% lower than base case. The difference between case 1 and case 2 is 0.43 kV/m. The change in CW at point C is most obvious. Case 1 is 26.54 m, which is 1.53% higher than base case. Case 2 is 24.86 m, which is 4.90% lower than base case. The difference between case 1 and case 2 is 1.68 m. It can be seen that the meteorological parameters have a great influence on the power frequency electric field.

3.3. Power Frequency Magnetic Field Analysis

The height of the calculation point to ground is 1.5 m. The horizontal range is between $-20 \sim +20$ m. The magnetic field intensity is calculated every 0.01 m horizontal distance. The magnetic field intensity distribution curves at three points are shown in Figure 3.

The distribution curve of the magnetic field intensity is unimodal distribution, presenting lateral attenuation trend with horizontal distance increasing. The maximum magnetic intensity M_{m} occurs at the center of the tower, which is different from electric field intensity. Overall, for the magnetic field intensity, case 2 is higher than base case, and case 1 is lower than base case. The closer to the tower,

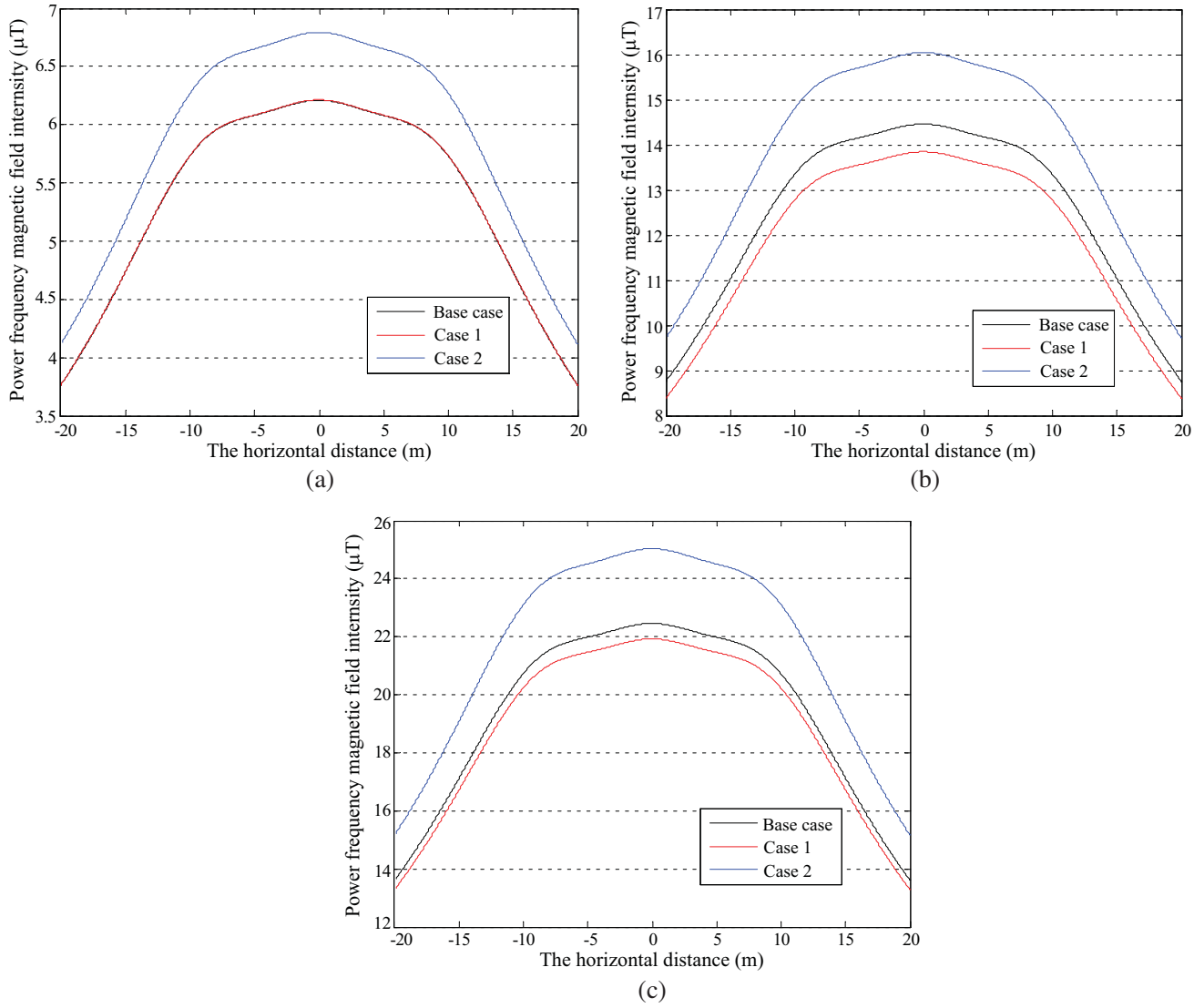

Figure 3. Power frequency magnetic field: (a) point A; (b) point B; (c) point C.

Table 5. M_{cw} and M_m under the three cases.

	Position	Base case	Case 1	Difference	Case 2	Difference
M_m (μT)	A	6.21	6.21	0	6.79	9.34%
	B	14.46	13.84	4.29%	16.05	11.0%
	C	22.46	21.93	2.36%	25.04	11.49%
M_{cw} (μT)	A	4.98	4.98	0	5.45	9.44%
	B	11.96	11.45	4.26%	13.27	10.95%
	C	18.65	18.21	2.36%	20.79	11.47%

the more obvious the phenomenon. The magnetic field intensity at the corridor boundary M_{cw} and the M_m are shown in Table 5. The corridor width is based on the value of base case.

The change in M_m at point B is most obvious. Case 1 is 13.84 μT, which is 4.29% lower than base case. Case 2 is 16.05 μT, which is 11% higher than base case. The difference between case 1 and case 2 is 2.21 μT. The change in M_{cw} at point B is most obvious. Case 1 is 11.45 μT, which is 4.26% lower than base case. Case 2 is 13.27 μT, which is 10.95% higher than base case. The difference between case 1 and case 2 is 1.82 μT. It can be seen that the meteorological parameters have a great influence on the power frequency magnetic field.

3.4. Radio Interference Analysis

The radio interference E_{RI} at the point, 20 m away from the side line and 2 m above the ground, is shown in Table 6. The change in E_{RI} at point C is most obvious. Case 1 is 47.97 dB, which is 2.76% higher than base case. Case 2 is 42.82 dB, which is 8.27% lower than base case. The difference between case 1 and case 2 is 5.15 dB. It can be seen that the meteorological parameters have a great influence on the radio interference.

Table 6. E_{RI} (dB) under the three cases.

Position	Base case	Case 1	Difference	Case 2	Difference
A	52.47	52.47	0	51.19	2.44%
B	47.32	47.97	1.37%	42.82	9.51%
C	46.68	47.97	2.76%	42.82	8.27%

4. CONCLUSIONS

The analysis method of meteorological parameters affecting the electromagnetic environment is presented in this paper. Meteorological parameters affect the conductor temperature, and then affect the line parameters. Overhead transmission line is the main component of power grids, and the variation of conductor temperature will have an impact on the system power flow. The changes of line voltage and current will affect the surrounding electromagnetic environment.

In the case study, the power frequency electric field, the power frequency magnetic field and the radio interference of IEEE 5-bus power system are studied. It can be seen that the meteorological parameters have a great influence on the electromagnetic environment around the line. The calculation of electromagnetic environment considering the changes of meteorological parameters is more accurate. In the future, the impacts of meteorological parameters on the electromagnetic environment of ultra-high voltage transmission lines under different sequence arrangements will be studied.

ACKNOWLEDGMENT

This paper is supported by the National Natural Science Foundation of China (No. 51607107, 51641702), and the Science & Technology Development Project of Shandong Province (No. ZR2015ZX045).

REFERENCES

1. He, J. L., S. M. Chen, J. Guo, R. Zeng, and J. Lee, "Electromagnetic environment analysis of a software park near transmission lines," *IEEE Transactions on Industry Applications*, Vol. 40, No. 4, 995–1002, 2004.
2. Okrainskaya, I. S., A. I. Sidorov, and S. P. Gladyshev, "Electromagnetic environment under over head power transmission lines 110–500 kV," *International Symposium on Power Electronics Power Electronics, Electrical Drives, Automation and Motion*, 796–801, 2012.
3. Zhao, L. X., J. Y. Lu, and G. F. Wu, "Measurement and analysis on electromagnetic environment of 1000 kV UHV AC transmission line," *IEEE Transactions on Industry Applications*, 1–4, 2012.
4. Sibanda, M., R. R. Van, and N. Parus, "Overview of the electromagnetic environment in the vicinity of HVDC transmission lines," *Proceedings of the 10th Industrial and Commercial Use of Energy Conference*, 1–7, 2013.
5. Wang, Y. L., Z. J. Yan, L. K. Liang, X. S. Han, and X. F. Zhou, "Dynamic rating analysis of overhead line loadability driven by meteorological data," *Power System Technology*, Vol. 42, No. 1, 315–321, 2018.
6. Zhang, H., X. S. Han, and Y. L. Wang, "Analysis on current carrying capacity of overhead lines being operated," *Power System Technology*, Vol. 32, No. 14, 31–35, 2008.
7. Douglass, D. A., "Weather-dependent versus static thermal line ratings," *IEEE Transactions on Power Delivery*, Vol. 3, No. 2, 742–753, 1998.
8. Heckenbergerova, J., P. Musilek, and K. Filimonenkov, "Assessment of seasonal static thermal ratings of overhead transmission conductors," *IEEE Power and Energy Society General Meeting*, 1–8, 2011.
9. Kim, S. D. and M. M. Morcos, "An application of dynamic thermal line rating control system to up-rate the ampacity of overhead transmission lines," *IEEE Transactions on Power Delivery*, Vol. 28, No. 2, 1231–1232, 2013.
10. Mo, Y., X. F. Zhou, Y. L. Wang, and L. K. Liang, "Study on operating status of overhead transmission lines based on wind speed variation," *Progress In Electromagnetics Research M*, Vol. 60, 111–120, 2017.
11. Wang, Y. L., Y. Mo, M. Q. Wang, X. F. Zhou, L. K. Liang, and P. Zhang, "Impact of conductor temperature time-space variation on the power system operational state," *Energies*, Vol. 11, No. 4, 1–15, 2018.
12. Wang, Y. F., H. Wang, H. Xue, C. Yang, and T. Yan, "Research on the electromagnetic environment of 110 kV six-circuit transmission line on the same tower," *IEEE PES Innovative Smart Grid Technologies*, 1–5, 2012.
13. CIGRE, "Thermal behavior of overhead conductors," CIGRE WG12, ELECTRA(144), 1992.
14. Grainger, J. J. and W. D. Stevenson, *Power System Analysis*, McGraw-Hill College, 1994.
15. Rakpenthai, C. and S. Uatrongjit, "Power system state and transmission line conductor temperature estimation," *IEEE Transactions Power Systems*, Vol. 32, No. 3, 1818–1827, 2017.
16. Huang, D. C., J. J. Ruan, and F. Huo, "Study on the electromagnetic environment of 1000 kV AC double-circuit transmission lines in China," *IEEE/PES Power Systems Conference and Exposition*, 1–7, 2009.
17. Huang, W. G., "Study on conductor configuration of 500 kV Chang-Fang compact line," *IEEE Transactions on Power Delivery*, Vol. 18, No. 3, 1002–1008, 2003.